A Numerical Computation of Gravity-Capillary Waves in Deep Water

Jang-Whan Kim and William C. Webster
Department of Naval Architecture & Offshore Engineering,
U.C. Berkeley

Introduction

The theoretical study on free-surface flow in a real fluid, which is governed by inertial, gravity, viscosity and surface tension, has been usually made with the last two physical parameters ignored. The effectiveness of this assumption depends on the length scale of the physical model for which the theory is applied. In the range of the length scales where the most hydrodynamic and oceanographic applications are made the simplified theory has been proven to be effective and practical. But there are some circumstances where the viscosity and surface tension can be no longer ignored. For the water waves with wave length comparable to 10cm, it has been known that the capillary waves with the short wave length ride on the carrier waves with the propagating speed comparable to the carrier gravity waves. Recently, Longuet-Higgins(1995) investigated this problem by considering the riding capillary waves as a perturbation due to the local action of surface tension forces on an otherwise pure gravity wave. He included the effect of viscosity in an empirical manner. He showed that for waves of wave length greater than 5cm there exists a critical steepness of the gravity wave at which the riding capillary wave exhibits a maximum amplitude. When the steepness of the gravity wave is lower than this critical value, capillary waves can be generated at all points of the wave surface. Otherwise, they are trapped between two caustics near the crests.

In this study we treat the same problem using direct numerical simulation. The most popular method for this kind of numerical simulation is the finite-difference method. But if one tries to apply this method to the present problem, adopting an adequate grid system to described the correct velocity profiles is difficult because there exist drastically different length scales raised by four distinct flow fields. Two of them are flow fields generated by the carrier gravity waves and the riding capillary waves, and the others are the flow fields due to the viscous boundary layer caused by the two wave components respectively. The depth-wise velocity profiles of the flow fields can be approximately described by exponential functions. With a given celerity C, the exponents for the wave components, k_{w1} and k_{w2} are determined by the dispersion relation of the gravity-capillary wave which can be written in terms of the gravity constant g and surface tension σ as follows

$$C = \sqrt{\frac{g + \sigma k_{wi}^{\,2}}{k_{wi}}}, \quad i = 1,2 . \tag{1}$$

The exponents for the boundary layer of each wave components are given as

$$k_{vi} = \sqrt{\frac{C k_{wi}}{2\nu}}, \quad i = 1,2 \tag{2}$$

where ν is the kinematic viscosity of the water. For the water wave of wave length 6.5cm, which is actually taken as a numerical example here, the four exponents have the relative values

$$\frac{k_{w2}}{k_{w1}} = 14.2, \quad \frac{k_{v1}}{k_{w1}} = 38.7, \frac{k_{v2}}{k_{w1}} = 145.7 , \tag{3}$$

which obviously show the diversity of length scales. Instead of applying a finite-difference method to the whole domain, we adopt the method of fluid sheet theory which has been widely used for nonlinear water wave theory (e.g., Shields & Webster, 1988).

Method of Solution

In the present method the continuity equation is satisfied exactly by describing the velocity field by a stream function $\psi(x,y,t)$. The stream function is expanded by depth-wise interpolation functions $\{\theta_i(\beta),\ i = 1,2,\ldots\}$ as

$$\psi(x,y,t) = \sum_i u_i(x,t)\,\theta_i(\beta(x,y;t)) \tag{4}$$

in a transformed coordinate system (x,β) defined as

$$\beta = \beta(x,y;t) = y - \eta(x,t). \tag{5}$$

where $\eta(x,t)$ is the free-surface elevation. The Navier-Stokes equations are weakly satisfied following the procedure of finite-element method given in Carey and Oden(1986) with an exception that the interpolation is made for the depth-wise direction only. The result can be written as

$$\begin{aligned}
&\left(1+\eta_x^2\right)A_{mn}^{11}u_{nt} - \eta_x A_{mn}^{10}u_{ntx} + A_{mn}^{10}\left(\eta_x u_{nt}\right)_x - A_{mn}^{00}u_{ntxx} = \\
&\eta_t\left(1+\eta_x^2\right)A_{mn}^{12}u_n - \eta_x A_{mn}^{11}\left(\eta_t u_n\right)_x - A_{mn}^{01}\left(\eta_t u_n\right)_{xx} + A_{mn}^{02}\left(\eta_x\eta_t u_n\right)_x - B_{mnk}^{111}u_n u_{kx} + B_{mnk}^{102}u_{nx}u_k \\
&-\eta_x\left\{\ B_{mnk}^{110}u_n u_{kxx} + B_{mnk}^{101}u_{nx}u_{kx} + B_{mnk}^{111}u_n\left(\eta_x u_k\right)_x - \eta_x B_{mnk}^{102}u_{nx}u_k\ \right\} \\
&-\left\{-B_{mnk}^{010}u_n u_{kxx} + B_{mnk}^{001}u_{nx}u_{kx} + B_{mnk}^{011}u_n\left(\eta_x u_k\right)_x - \eta_x B_{mnk}^{002}u_{nx}u_k\right\}_x \\
&-\nu\Big[\ -4A_{mn}^{11}u_{nxx} + 4A_{mn}^{12}\left(\eta_x u_n\right)_x - 4\eta_x A_{mn}^{21}u_{nx} + 4\eta_x^2 A_{mn}^{22}u_n \\
&\qquad +(1-\eta_x^2)\left\{(1-\eta_x^2)A_{mn}^{22}u_n - A_{mn}^{20}u_{nxx} + A_{mn}^{21}\left(\eta_x u_{nx} + (\eta_x u_n)_x\right)\right\} \\
&+\left(\eta_{xx} + 2\eta_x\frac{\partial}{\partial x}\right)\left\{(1-\eta_x^2)A_{mn}^{12}u_n - A_{mn}^{10}u_{nxx} + A_{mn}^{11}\left(\eta_x u_{nx} + (\eta_x u_n)_x\right)\right\}\ \Big] \\
&-\left\{p + g\eta - \frac{\sigma\eta_x}{\left(1+\eta_x^2\right)^{3/2}}\right\}_x \theta_m(0) + \tau(1+\eta_x^2)\dot{\theta}_m(0) + (\tau\eta_x)_x\theta_m(0)
\end{aligned} \tag{6}$$

where $p(x,t)$ and $\tau(x,t)$ are the pressure and the tangential shear stress on the free surface, respectively. The coefficients $A_{mn}^{\alpha\beta}$ and $B_{mnk}^{\alpha\beta\gamma}$ are defined as

$$A_{mn}^{\alpha\beta} = \int_{-\infty}^{0} D^\alpha\theta_m(\eta)\,D^\beta\theta_n(\eta)\,d\eta, \tag{7.a}$$

$$B_{mnk}^{\alpha\beta\gamma} = \int_{-\infty}^{0} D^\alpha\theta_m(\eta)\,D^\beta\theta_n(\eta)D^\gamma\theta_k(\eta)\,d\eta \tag{7.b}$$

where D is the differential operator. It should be noted that the above equation can be also derived by the fluid sheet theory.

Numerical Results

Computations are made for waves generated by a pulsating pressure patch. The free surface conditions are given as

$$p(x,t)=\begin{cases}\dfrac{P_{\max}}{2}\cos^2\left(\dfrac{\pi x}{L}\right)\sin\omega t, & -\dfrac{L}{2}\le x\le\dfrac{L}{2}\\ 0, & \textit{otherwise}\end{cases} \tag{8.a}$$

$$\tau(x,t)=0 \tag{8.b}$$

where L is taken as the wave length and the circular frequency ω is taken such that the generated gravity waves have the wave length of 6.5cm. For the depth-wise interpolation, nine functions are taken as

$$\theta_i(\beta)=\beta^{m_i}\exp(k_i\beta) \tag{9}$$

with

i	m_i	$k_iL/2\pi$
1	0	1
2	1	1
3	2	1
4	1	14.2
5	2	14.2
6	1	38.7
7	2	38.7
8	1	145.7
9	2	145.7

Here, the exponents of the interpolation functions are taken from Eqs. (1) and (2). Finite difference method is used to discretize Eq.(6) in x-direction with a uniform mesh of 200 nodes per wave length. The 4th-order Runge-Kutta method is used for the time integration. Computations are made for the following magnitudes of pressure patch,

$$\frac{P_{\max}}{\rho gL}=0.15,0.16,\ldots,0.20. \tag{10}$$

and wave elevation and its slope is measured at four locations, $x = L,\ 2L,\ 3L,\ 4L$. It has been found that the numerical results show a good agreement with the experimental result of Cox(1958). In Fig.1 time history of wave slopes computed with $\frac{P_{\max}}{\rho gL}=0.15$ and 0.20 are compared. It can be found that the generation of capillary waves are more significant when the amplitude of the carrier gravity wave is higher. Fig.2 shows the profile of wave slope at $t = 8T$ where T denotes the period of the gravity wave. The capillary wave shows significant decay along the x-direction, presumably due to viscous dissipation.

References

Carey, G.F. and Oden, J.T. 1986 FINITE ELEMENTS: Vol VI. Fluid Mechanics, Prentice-Hall.

Cox, C.S. 1958 "Measurements of Slopes of High-Frequency Wind Waves," J. Mar. Res., Vol. 16, pp. 199-225.

Longuet-Higgins, M.S. 1995 "Parasitic Capillary Waves: a Direct Calculation," J. of Fluid Mech., Vol. 301, pp. 79-107.

Shields, J. J. and Webster, W. C. 1988 "On Direct Methods in Water-Wave Theory," J. of Fluid Mech., Vol. 197, pp. 171-199.

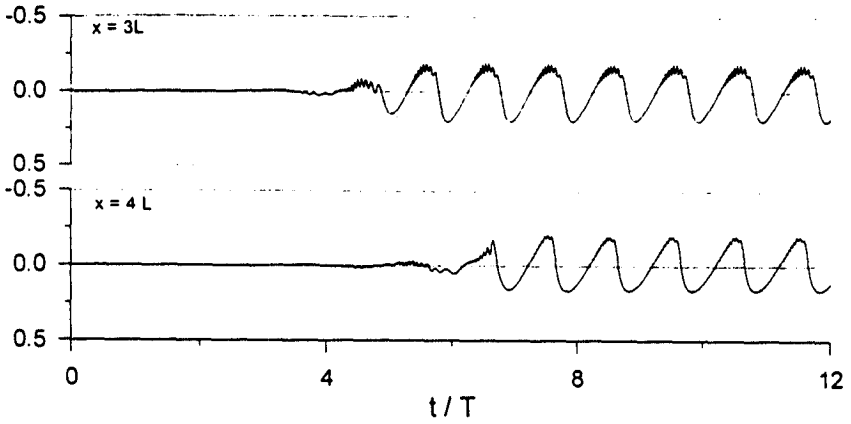

(a)

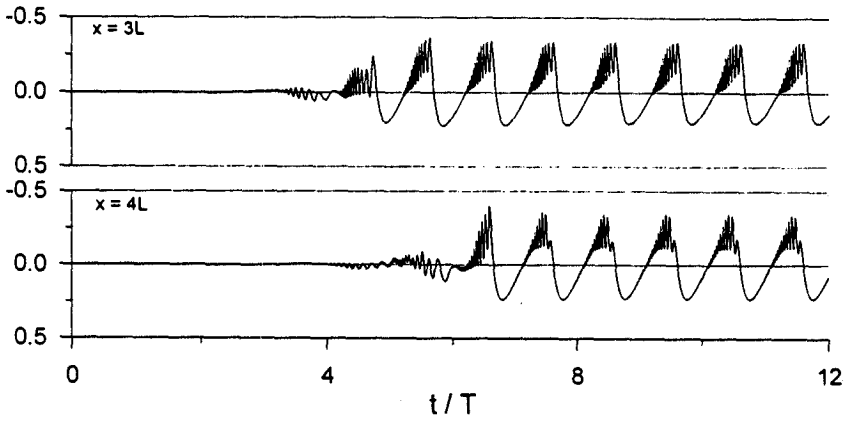

(b)

Fig.1 Time history of wave slopes.
(a) $\frac{P_{max}}{\rho g L} = 0.15$ (b) $\frac{P_{max}}{\rho g L} = 0.20$

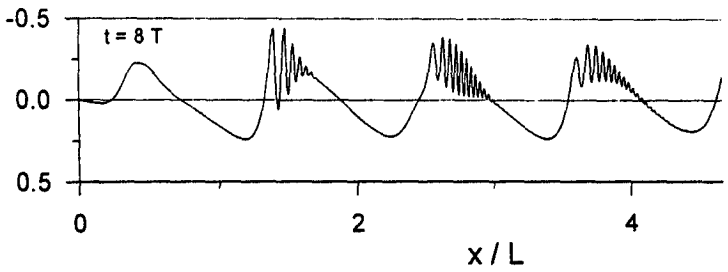

Fig.2 Wave profile at t = 8T. $\frac{P_{max}}{\rho g L} = 0.20$.

DISCUSSION

Takagi: I think that the choice of the depthwise interpolation function may affect the results. How did you decide the depthwise interpolation function?

Kim & Webster: There are several choices of depthwise interpolation functions (or basis functions). These functions include polynomials, sinusoidal functions, and exponential functions. These functions are such that a finite set of them is closed under differentiation. The selection of which type of function to use is made by considering the likely variation in velocity with depth. That is, the "shape" of the velocity profiles expected should be able to be described by some combination of the basis functions. There is no maximum number of basis functions which can be used. Each selection results in a separate theory. The presumption is that the more basis functions which are selected, the more accurate the results, since the real kinematics can be more closely monitored. In fact, it can be shown that this is the case.